

TWO-DIMENSIONAL WAVE OVERTOPPING CALCULATION OVER A DIKE IN SHALLOW FORESHORE BY SWASH

Tomohiro Suzuki^{1,2}, Corrado Altomare^{1,3}, Toon Verwaest¹, Koen Trouw⁴ and Marcel Zijlema²

In this paper, a numerical wave-flow model SWASH, based on non-linear shallow water equation with non-hydrostatic pressure, is applied to the estimation of wave overtopping over a dike in shallow foreshores. First sensitivity analysis is conducted to see the influence of wave generation, grid size, time window and bottom friction by one-dimensional calculations. After that the SWASH model is validated by comparing results from field measurements in Petten dike in the Netherlands. Due to the stability of the computation, the desired calculation could not be achieved, but an alternative way to calculate wave overtopping including two-dimensional effects is proposed.

Keywords: SWASH model; wave overtopping; directional spreading; free long waves; shallow foreshores

INTRODUCTION

The potential of sea level rise and increasing storminess are threats for coastal areas. For actual designs such as construction of storm walls and implementation of beach nourishment as the countermeasures of the extreme storms for the coastal safety, an appropriate estimation of wave overtopping is necessary. In the case of deep water conditions with simple dike configurations, the estimation methods for the wave overtopping have been well developed (e.g. EurOtop, 2007). On the other hand, estimation methods for the wave overtopping in shallow foreshore condition (e.g. Van Gent, 1999) are limited in applications compared to ones for deep water conditions. Also, there is an uncertainty for the two-dimensional effect for the wave overtopping in the shallow foreshore condition: a recent numerical study (Guza and Feddersen, 2012) shows that the directional spreading, in other words short-crestedness of the waves, influences the run-up height. It indicates that the wave overtopping calculation in the shallow foreshore condition must account for the two-dimensional effects.

In practice, wave overtopping discharge is calculated by empirical formulas (e.g. EurOtop, 2007; Mase et al., 2013) using wave boundary conditions. Wave boundary conditions are typically estimated using physical models and numerical models. Physical models give a reliable estimation of wave boundary conditions, still considerable time and resources are necessary. Even it is feasible, for instance, bathymetric changes in physical model are often difficult to be implemented in practice: the bottom of the model, often consisting of concrete works, has to modify/re-construct case to case. Therefore the demand/expectation of numerical models is getting higher these days. However, still numerical models do not always represent wave transformation processes accurately, especially in shallow foreshores: free long waves occur since the group bounded waves (e.g. Ottesen-Hansen et al., 1980; Barthel et al., 1983) in the wave train in the offshore are released in the shallow zone through wave breaking and wave-wave interactions. For example spectral wave models cannot reproduce the free long waves since frequency shift due to those phenomena in the breaking zone cannot be modeled properly. Capability of the accurate estimation of the free long waves is a key for the good estimation of the wave overtopping discharge in the shallow foreshore condition over a dike. Even though appropriate wave boundary conditions (e.g. at toe of the dike) for wave overtopping are obtained, not always the existing formulas are applicable to the local dike geometries. Also the obtained spectrum at the boundary has often two peaks due to the generation of the free long waves, which make more difficult to apply existing formulas.

To overcome these difficulties, it is desirable to have a numerical model which is capable to calculate wave transformation and wave overtopping together. For the calculation of the free long waves, phase-resolving wave models seem to be suitable since they are capable to deal with wave frequency shift due to wave breaking and wave-wave interaction. Instantaneous wave overtopping discharges, which can be obtained from phase-resolving wave models, are also useful information for the actual coastal defense design since maximum layer thickness and speed of one overtopping wave

¹ Flanders Hydraulics Research, Berchemlei 115, 2140 Antwerp, Belgium, tomohiro.suzuki@mow.vlaanderen.be

² Environmental Fluid Mechanics Section, Faculty of Civil Engineering and Geosciences, Delft University of Technology, P.O. Box 5048, 2600 GA Delft, The Netherlands.

³ Dept. of Civil Engineering, Ghent University, Technologiepark 904, 9052 Ghent, Belgium

⁴ Fides Engineering, Sint Laureisstraat 69d, 2018 Antwerp, Belgium

can be more relevant for the detailed design (e.g. force acting on the structure) rather than only mean wave overtopping discharge. Still, to conduct such a calculation, the model should be computationally not too demanding and stable since the computation can be relatively long (e.g. 1000 waves) and the dimension can be large especially in two-dimensional calculations.

Recently a phase-resolving wave propagation model, SWASH (Zijlema et al., 2011), based on the non-linear shallow water equations with a non-hydrostatic pressure term has been developed at the Delft University of Technology. The model is a depth integrated model, thus the computational cost is not very high. Due to the shock capturing feature of the non-linear shallow water equations wave breaking effect is calculated accurately without adding any additional terms in the basic equations. To avoid a high vertical resolution SWASH uses hydrostatic front approximation for the wave breaking (Smit et al., 2014). On the other hand, the wave breaking in typical Boussinesq type equation models need to be modeled by artificial wave dissipation terms. Recent development of generation of infra-gravity waves in the SWASH model by Rijnsdorp (2014) enables to generate the second-order waves which is important for the accurate generation of the group bounded waves: it influences the wave transformation. Furthermore, the usefulness of the SWASH model is not limited to the accuracy of the model but also the computational efficiency. The parallel computation function makes it easier to apply relatively long time duration and large domain. Suzuki et al. (2011) has already demonstrated that this model produces satisfactory results for both wave transformation and wave overtopping in shallow foreshore in their one-dimensional calculation. Also, Suzuki et al. (2012) showed the capability of two-dimensional calculation for wave penetration in a marina.

In this study, we extend these studies to see the applicability of SWASH to a two-dimensional wave overtopping calculation over a dike in a shallow foreshore.

NUMERICAL MODEL

The SWASH model is a time domain model for simulating non-hydrostatic, free-surface and rotational flow. The governing equations are the non-linear shallow water equations including a non-hydrostatic pressure term. The two-dimensional, depth-averaged shallow water equations are shown as follows:

$$\frac{\partial u}{\partial x} + \frac{\partial v}{\partial y} + \frac{\partial w}{\partial z} = 0 \quad (1)$$

$$\frac{\partial u}{\partial t} + \frac{\partial u^2}{\partial x} + \frac{\partial vu}{\partial y} + \frac{\partial wu}{\partial z} + \frac{g}{\rho_0} \frac{\partial \zeta}{\partial x} + \frac{g}{\rho_0} \frac{\partial q}{\partial x} + c_f \frac{u|u|}{h} = \frac{1}{h} \left(\frac{\partial h\tau_{xx}}{\partial x} + \frac{\partial h\tau_{xy}}{\partial y} \right) \quad (2)$$

$$\frac{\partial v}{\partial t} + \frac{\partial uv}{\partial x} + \frac{\partial v^2}{\partial y} + \frac{\partial wv}{\partial z} + \frac{g}{\rho_0} \frac{\partial \zeta}{\partial y} + \frac{g}{\rho_0} \frac{\partial q}{\partial y} + c_f \frac{v|v|}{h} = \frac{1}{h} \left(\frac{\partial h\tau_{yx}}{\partial x} + \frac{\partial h\tau_{yy}}{\partial y} \right) \quad (3)$$

$$\frac{\partial w}{\partial t} + \frac{1}{\rho_0} \frac{\partial q}{\partial z} = 0 \quad (4)$$

$$\tau_{xx} = 2\nu_t \frac{\partial u}{\partial x}, \tau_{xy} = \tau_{yx} = \nu_t \left(\frac{\partial v}{\partial x} + \frac{\partial u}{\partial y} \right), \tau_{yy} = 2\nu_t \frac{\partial v}{\partial y} \quad (5)$$

where t is time, x and y the horizontal coordinate, z the vertical coordinate, u , v and w the velocity in x -direction, y -direction and z -direction respectively. ζ is the surface elevation from still water level and h is the total depth. q is the non-hydrostatic pressure, g the gravitational acceleration, c_f is the dimensionless bottom friction coefficient and ν_t the local effective viscosity.

A full description of the numerical model, boundary conditions, numerical scheme and applications are given in Zijlema et al. (2011).

MODEL SETTINGS

In situ measurement setup

In this study, in-situ measurement data set from Petten sea-defence in The Netherlands is used to validate wave overtopping calculation by SWASH. Rijkswaterstaat had conducted continuous measurement such as the water level, wind, wave propagation, wave run-up and wave overtopping discharge until 2013 (D. Slagter, personal communication, 6th January 2014). Wave overtopping events

were observed several times, and one of which was on 9th November 2007. The data set obtained at 03:20 a.m. on that day has been applied to this study.

The wave directional spreading and wave direction are measured at directional wave buoys 011 and 021, both located much offshore from 031. The water surface time series is measured at wave directional buoys 011, 021, and also at wave buoys 031, 161, 171, 181, 061 and 071, see Figure 1.

The sampling frequency of the wave buoy data is 4.00 Hz at the wave buoys 031, 161, 171, 181, 061 and 071, and 2.56 Hz at the directional wave buoys 011, 021 and 031. Wave overtopping data are recorded when a wave overtopping by one wave occurs at wave overtopping tank at 091. The beginning time, the ending time and the wave overtopping volume of an individual wave are available. Therefore number of the wave overtopping in the unit time duration is available. The post-processed data for the wave parameters and the wave spectrum, both based on 20 minutes time series, are also available. However the raw data are re-analyzed by us to be able to see the detailed information on low-frequency waves in this study since the low frequency wave data is cut off at 0.03 Hz during the post-processing mainly to remove the influence of the tide.

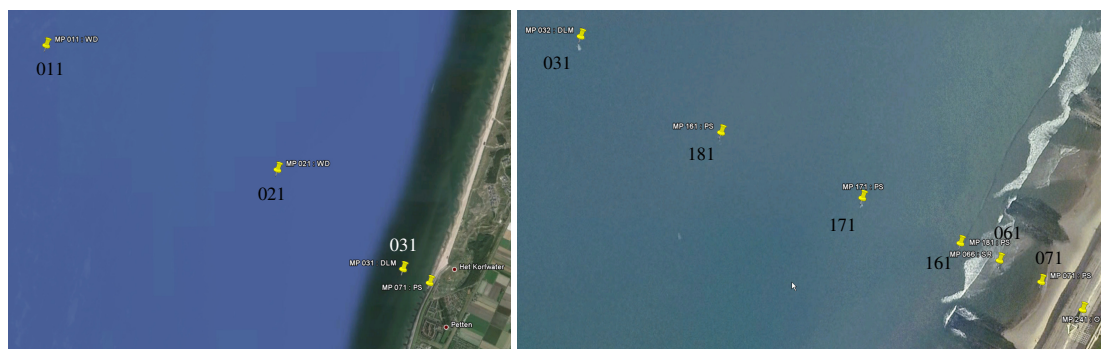


Figure 1. Pictures of measurement points in Petten

Numerical model setup

Two-dimensional wave overtopping calculation over a dike in shallow foreshore is conducted by SWASH (version 2.00). Even though the purpose of this study is to test two-dimensional calculations for wave overtopping, both one-dimensional and two-dimensional calculations are tested to see the characteristics of wave overtopping in each case. One layer is used for the number of vertical layers since the kd value (k is the wavenumber) at the wave boundary in the model is small enough: it is assumed that the one layer model still resolve the frequency dispersion in an acceptable level in case of $kd < 1.4$. And also, one-dimensional computation is more stable than two-dimensional computation in the case of wave overtopping calculation from the authors' experiences.

The wave boundary conditions used in the model runs are shown in Table 1. The wave height H_{m0} is 4.6 m which is close to the value observed at the deep water wave buoy at 031 while the peak wave period T_p is set as 11.0 s taking into account the offshore buoy spectral period $T_{m-1,0}$ which is 9.56 s at 021 assuming wave period is constant from offshore in the deep water. A JONSWAP spectrum with $\gamma=2.5$ is used to be able to get similar offshore wave spectrum shape in the calculations. Seed number which decides the time series of waves is fixed when a sensitivity test is conducted. It is important to use the same wave train for the sensitivity analysis since wave train can influence wave overtopping discharge (Williams et al., 2014). The wave direction at 03:20 is NW, which is almost perpendicular direction to the dike. Therefore the wave main direction is set at 0 degree, i.e. perpendicular to the dike, in the simulations. In this way one-dimensional and two-dimensional calculation can be compared in a fair way. The directional spreading is set at 22.4 degree taking into account the directional spreading data measured at 011 and 021. Normally directional spreading data at 021 would be the most appropriate value for the wave boundary in the domain defined in this study, but the directional spreading data is missing at 021 at 03:20. Therefore, data at 011 at 03:20 is used to obtain the directional spreading by using the relationship between 011 and 021. Concretely, the directional spreading at 03:20 at 011 is 27 degree and the difference of the average directional spreading between 011 and 021 is 4.6 degree in one set of data. The wave generation is based on the second-order waves so that the parasitic waves can be eliminated (e.g. Ottesen Hansen et al. 1980; Barthel et al., 1983). A weakly-reflective boundary is applied at the wave boundary, and the Sommerfeld radiation condition is

applied at the end of the numerical domain, in order to minimize the effect of the reflection. The initial time step is set 0.01 s. Note that the calculation time step is automatically adjusted in the calculation depending on the CFL condition. In this study a maximum CFL value of 0.5 is used. As for the numeric, non-hydrostatic pressure is included. As indicated in Suzuki et al. (2011), the non-hydrostatic pressure plays an important role in the wave propagation. The Keller box scheme is applied since it is one layer calculation. The time duration of the numerical simulations is 20 minutes which are the same time length as used in the post-processing for the in-situ measurement.

The bathymetry data just after the storm of 9th November 2007 (dated on 15th November 2007) is also available. Figure 2 shows the bathymetry data in the cross section of the wave buoys from 071 to 031, which direction is about perpendicular to the dike and between WNW to NW, see Figure 1. The dike crest level in the figure was set at +6.7 m NAP, which is the top level of the wave overtopping box and the configuration of the dike behind the wave overtopping box is not representing the local geometry since this part is optimized for the model runs. The toe of the dike is located at 921 m distance from the wave boundary in the x-direction, which corresponds to the wave buoy 071. The same cross section is applied to the along-shore direction for the simplicity while the reality is somewhat different than one shown in Figure 3. A Manning's n value of 0.019 was used as a bottom friction in the numerical model runs.

The two-dimensional calculation domain is shown in the left figure in Figure 3. The unit of the level is m NAP. The domain size is 1200 m in x-direction and 1600 m in y-direction. The domain size of y-direction is set long enough not to be influenced by the side boundary of the model. Since the boundary condition at the side walls are set as closed boundaries, the waves are reflected at the side boundary and thus the wave height distribution is almost uniform in y-direction as shown in the right figure in Figure 3, which indicates the wave field for the estimation of wave overtopping is successfully obtained in the cross sections in the middle of the domain.

Wave overtopping discharge is calculated directly using time varying layer thickness $h(t)$ and layer speed $u(t)$ at the end of the dike in the SWASH model (Suzuki et al. 2011). The instantaneous wave overtopping $q(t)$ and the mean overtopping discharge q_{mean} are calculated by the following equations.

$$q(t) = h(t)u(t) \quad (6)$$

$$q_{1D} = \int_{t_s}^{t_e} q(t)dt / (t_e - t_s) \quad (7)$$

where t_s and t_e are start and end time of the wave overtopping measurement, respectively. This is the methodology to obtain wave overtopping discharge for one-dimensional calculation and long crested waves in two-dimensional calculation. In the case of short crested waves in the two-dimensional calculation, the wave overtopping discharge is not uniform. To have a reliable value, spatial averaging is applied to obtain representative wave overtopping discharge as follows. In this study, 11 points are selected ($m=11$) as shown in Figure 3 (white points).

$$q_{2D} = \sum_{n=1}^m \int_{t_s}^{t_e} q_n(t)dt / (t_e - t_s) / m \quad (8)$$

Further detailed settings (e.g. number of the grids; time window for the wave analysis; bottom friction settings) are discussed in the next section, sensitivity analysis.

Table 1. The offshore wave condition employed at the wave boundary in the simulation						
Date	Time	SWL	H_{m0}	T_p	Dir spr.	Direction
[-]	[-]	[m NAP]	[m]	[s]	[deg]	[deg]
09/11/2007	03:20	2.82	4.6	11.0	22.4	0.0

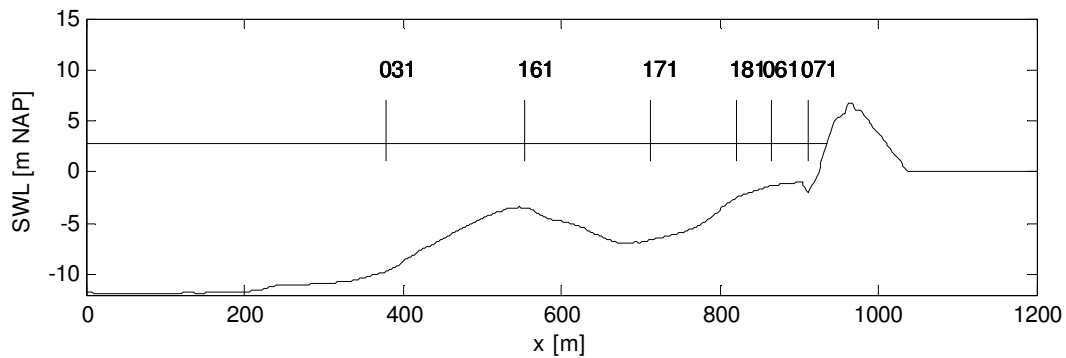


Figure 2. Topography and wave measurement positions. The bathymetry measurement was on 15/11/2007, after the storm of 09/11/2007.

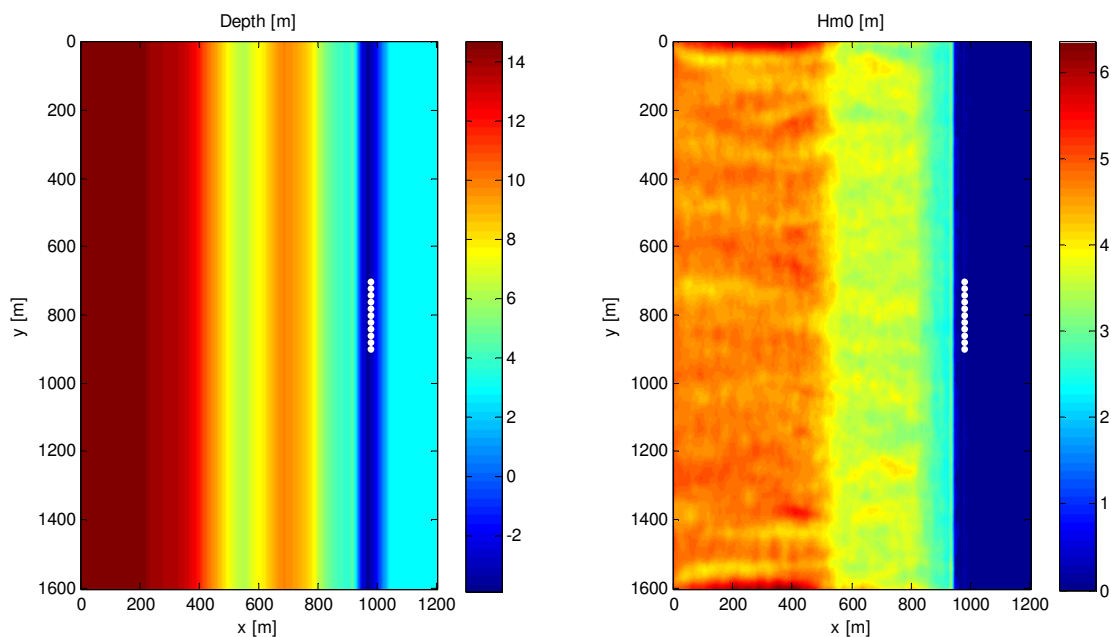


Figure 3. Water depth from SWL for two-dimensional calculation (left) and the significant wave height distribution (right).

SENSITIVITY ANALYSIS

First-order vs. second-order waves in one-dimensional calculation

To see the difference of wave overtopping discharge in different wave generation accuracy, namely the first-order and the second-order wave generation, a comparison has been made in one-dimensional calculations with the grid size of 2.0 m. The wave boundary conditions are based on the values shown in Table 1 except the directional spreading for this sensitivity analysis: directional spreading value here is 0 degree since it is one-dimensional calculation.

Figure 4 shows the wave transformation from the offshore wave buoy 031 to the wave buoy 071, at the toe of the dike. Both wave spectrum at 031 more or less correspond each other except the low frequency energy. Difference is clearer at 071. The wave spectrum around the peak period and the low-frequency part is overestimated in the first-order case. This leads overestimation of significant wave height at the toe of the dike and wave overtopping discharge as shown in Table 2. Note that the significant wave height here is total wave height, not incident wave height. Therefore this value cannot directly apply to the overtopping formulae.

Wave generation	Dx	H _{m0} at 071	Overtopping
[-]	[m]	[m]	[l/m/s]
First-order	2.0	2.92	5.6
Second-order	2.0	2.77	0.0

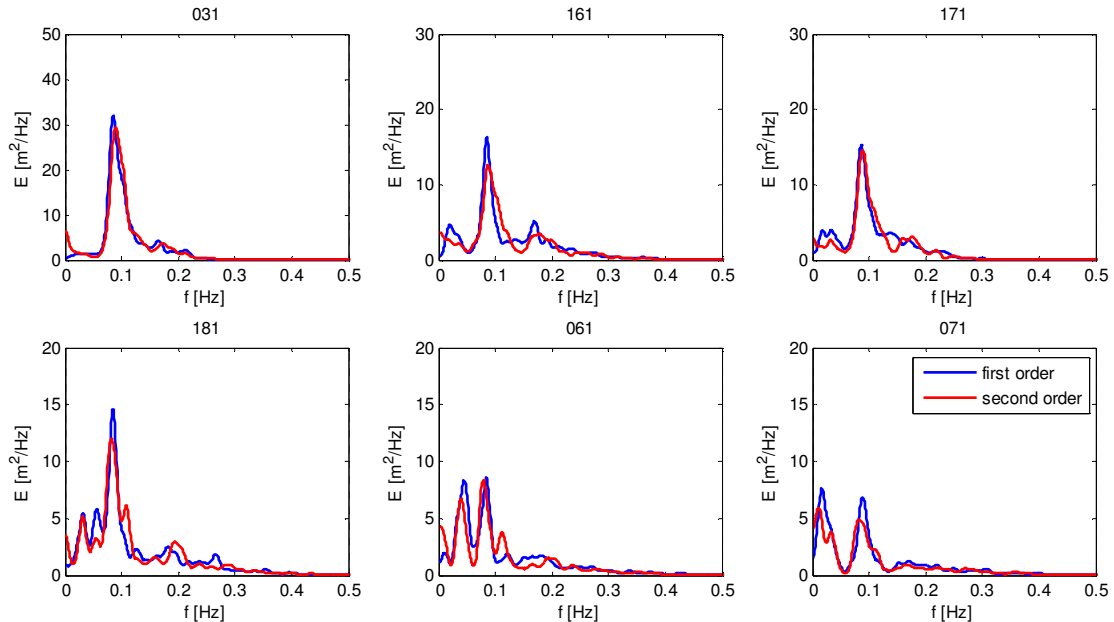


Figure 4. Computed wave spectrum in the first order wave generation (blue) against one in the second order wave generation (red).

Time window for wave analysis

In the in-situ measurement, the wave time series are continuously measured while a time window of 20 minutes is used to process the wave parameters. In the wave overtopping simulation in the SWASH model here, also 20 minutes calculation is used to be able to compare with the in-situ measurement. However, the SWASH model calculation needs to take some time to develop certain wave fields in the domain since it starts from still water condition; no waves at the beginning. Therefore the duration of each calculation is set as 30 minutes.

In this section the time window, the beginning time and the ending time, for the process of the wave parameters and wave overtopping discharge is discussed. Two time windows (200 – 1400 s and 600 – 1800 s) are compared in one-dimensional calculations with the grid size of 2.0 m.

The results show that the wave spectrum (Figure 5) and wave height (Table 3) at 071, at the toe of the dike, does not change so much. On the other hand, the wave overtopping discharge is observed around 400 s (Figure 6). That is why the result of wave overtopping discharge is different. However the first wave overtopping phenomena would be somewhat different from the reality: the first wave overtopping in the simulation is under the dry bottom. From author's experience, the first wave overtopping discharge in general would give higher overtopping discharge. The first wave overtopping appears in a stochastic manner, so it is difficult to fix the time window, but in this study the time window of 600-1800 s is used.

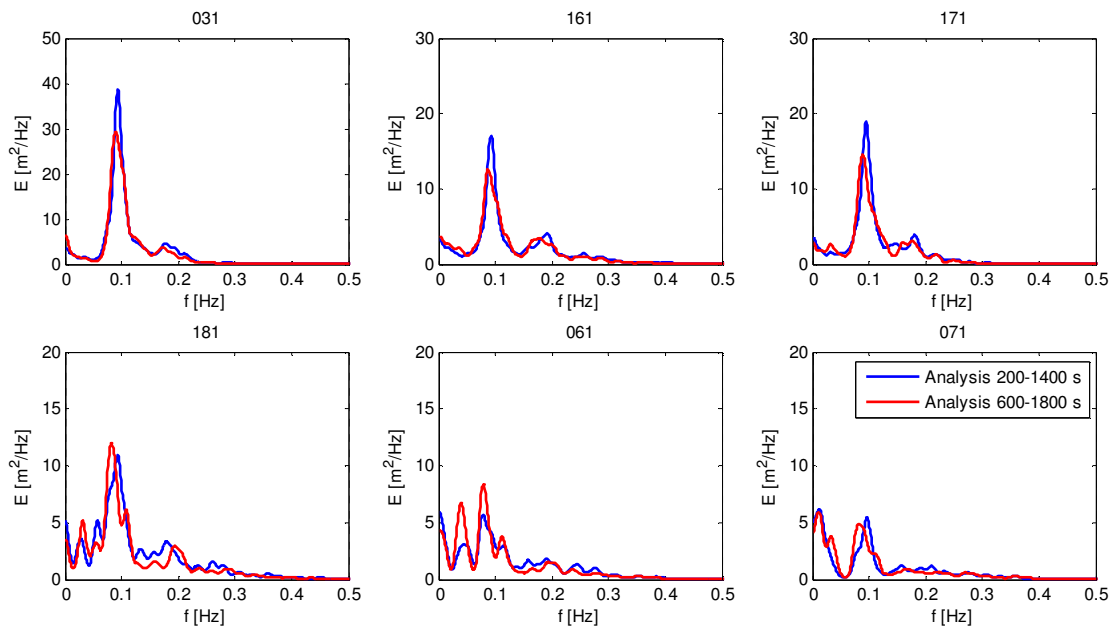


Figure 5. Computed wave spectrum analyzed in 200-1400 s (blue) against one in 600-1800 s (red).

Wave generation [-]	Dx [m]	H _{m0} at 071 [m]	Overtopping [l/m/s]
200-1400 s	2.0	2.73	0.1
600-1800 s	2.0	2.77	0.0

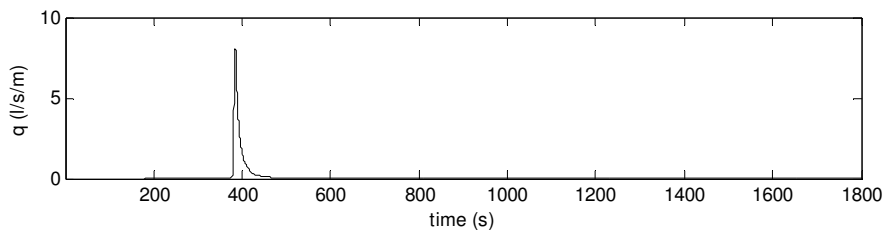


Figure 6. Time series of instantaneous wave overtopping discharge.

Grid size

The sensitivity of grid size in x-direction/cross-shore direction is investigated in one-dimensional calculations. Only the grid size in cross-shore direction is investigated since the grid size is important for the wave propagation, wave run-up and overtopping. We assume along-shore resolution does not play an important role for those phenomena since the directional spreading at the toe of the dike must be small.

Figure 7, Figure 8 and Table 4 shows a comparison of wave spectrum, wave height and wave overtopping discharge among those grid sizes. Note that the offshore wave height at 031 is calibrated (input values are slightly different for each cases) to be able to compare those wave propagation equally. It is clear that the influence of the grid size to the wave transformation is somewhat limited: wave height is slightly increased by the grid size. On the other hand the results shown in Table 4 indicate that the grid size influences the wave overtopping significantly. The wave overtopping discharge is increased when the grid size becomes smaller until 0.5 m. It seems that the wave overtopping discharge saturates when grid size becomes 0.5 m.

To be able to see more insight, the incident wave height is increased for the one test case since the wave overtopping discharge is closely related to the incident wave height. The slight change might lead big difference in wave overtopping discharge. Table 5 shows the comparison of the wave overtopping discharge between different incident wave heights. The result shows there is no wave overtopping

discharge in both cases. The wave overtopping is in general sensitive to the wave height at the toe of the dike, however in this specific case, the grid size change from 2 m to 0.5 m gives more influence on wave overtopping than the change of wave height at the toe of the dike from 2.77 to 2.91 m.

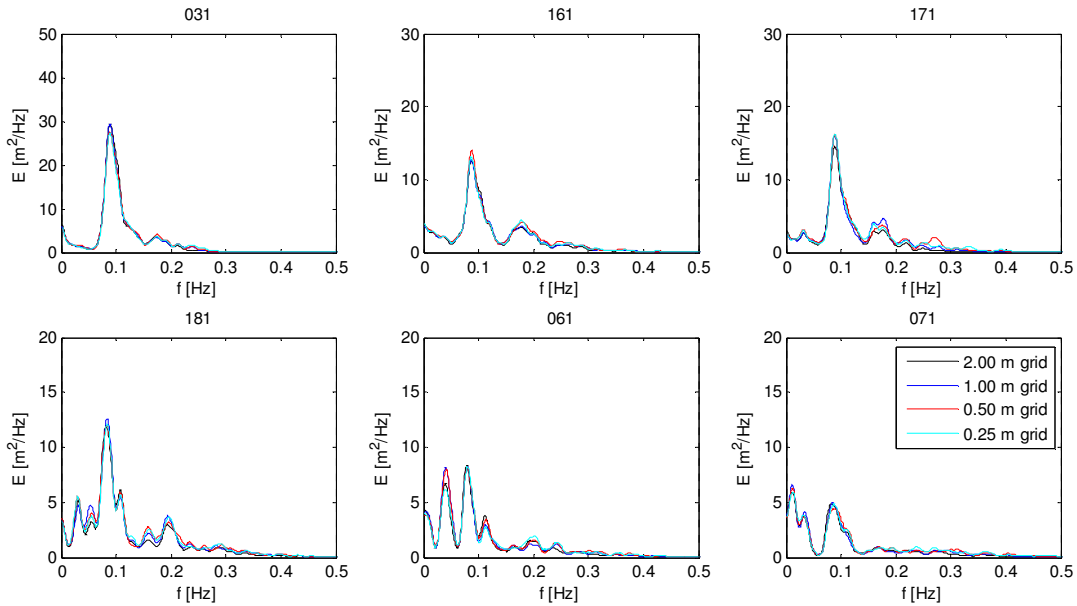


Figure 7. Comparison of wave spectrum among different grid sizes.

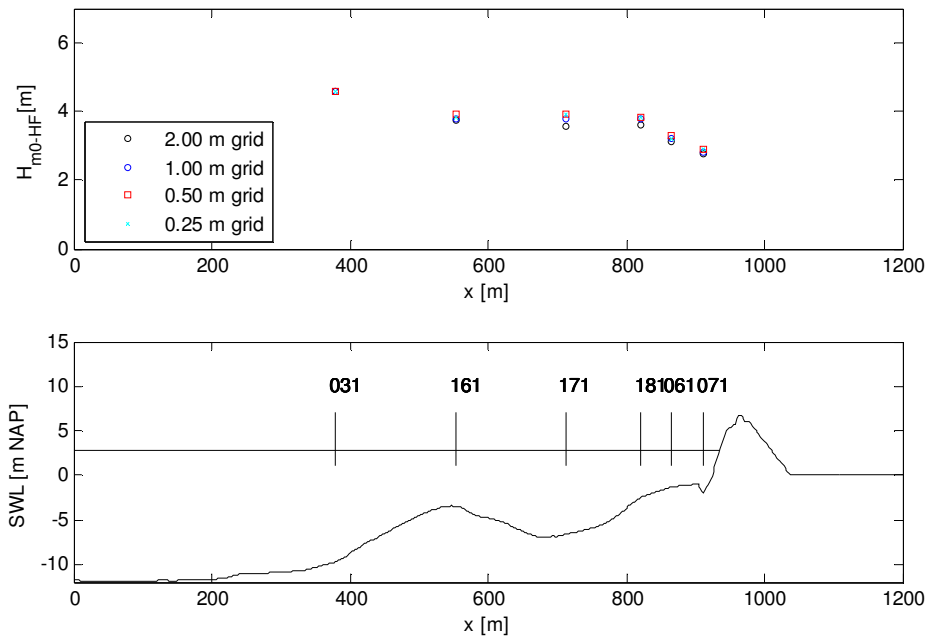


Figure 8. Wave height distribution in different grid sizes.

Table 4. Wave overtopping discharge in the different grid sizes				
Dx [m]	Input H_{m0} [m]	H_{m0} at 031 [m]	H_{m0} at 071 [m]	Overtopping [l/m/s]
2.0	4.60	4.60	2.77	0.0
1.0	4.50	4.61	2.83	2.2
0.5	4.49	4.61	2.89	5.9
0.25	4.42	4.57	2.91	4.3

Input H_{m0} [m]	Dx [m]	H_{m0} at 031 [m]	H_{m0} at 071 [m]	Overtopping [l/m/s]
4.60	2.0	4.60	2.77	0.0
5.20	2.0	5.13	2.91	0.0

Bottom friction

The sensitivity of bottom friction is investigated in one-dimensional calculations with the grid size of 0.5 m. The bottom friction to be used for this sensitivity analysis are 0.000 (no friction) and 0.019 (default Manning's bottom friction value in SWASH).

Table 6 shows a comparison of wave height and wave overtopping discharge in the different bottom friction. The same wave height is obtained at 071. This indicates that the bottom friction does not influence to the wave transformation. On the other hand the wave overtopping discharge is changed by the bottom friction. Not only the overtopping discharge but also the number of overtopping events in 20 min is also different.

Bottom frictions [-]	Dx [m]	H_{m0} at 071 [m]	Number of overtopping [times/20 min]	Overtopping [l/m/s]
0.000	0.5	2.89	24	13.4
0.019	0.5	2.89	15	5.9

VALIDATION

Preliminary two-dimensional wave overtopping calculation

In two-dimensional calculation, the directional spreading effect is included directly. As a preliminary test, grid size of 2 m in x-direction and 4 m in y-direction is used to see the two-dimensional wave overtopping discharge. Then the result of wave overtopping discharge is compared to the Petten in-situ measurement.

Figure 9 shows wave transformation from offshore to toe of the dike. Blue, red, black lines show one-dimensional calculation (i.e. the directional spreading of 0 degree), two-dimensional calculation (i.e. the directional spreading of 22 degree) and the in-situ measurement, respectively. The one-dimensional calculation is conducted to see the effect of the directional spreading. As can be seen in the figure, the wave spectrum of two-dimensional calculation shows a good correspondence with the measurement at 071 even though the value around the peak period is slightly underestimated. On the other hand, the one-dimensional calculation is overestimated at the low-frequency part while similar spectrum to the two-dimensional calculation is obtained around the peak period.

Table 7 shows the wave overtopping discharge for each calculation. The wave overtopping is not observed in the 2 m grid calculation both for 1D and 2D calculation. As shown in the sensitivity analysis, the grid size influences the wave overtopping discharge. Therefore the two-dimensional wave overtopping calculation is conducted using 0.5 m grid size, which seems to be the optimum grid size in this study case. In the next section the two dimensional calculation with 0.5 m grid is tested.

Two-dimensional wave overtopping calculation

The grid size of 0.5 m in x-direction and 0.5 m in y-direction is used to see the two-dimensional wave overtopping discharge. However, due to the instability of the computation, the result has not been obtained. It seems that the computation becomes more unstable when the grid size becomes smaller. The reason for this is unknown and should be investigated in the near future.

Alternative wave overtopping calculation including directional spreading effect

Since the computation is not completed due to the instability of the model, an alternative method is proposed here. The alternative method is a combination of two-dimensional calculation and one-

dimensional calculation: the two-dimensional calculation is for the wave transformation and the one-dimensional calculation is for the wave overtopping.

From the sensitivity analysis, the wave transformation does not change so much in the different grid size. However, the wave transformations in the one-dimensional and two-dimensional are different in the shallow foreshore case as can be seen in the difference in the spectrum at 071 in Figure 9. Therefore it is important to use two-dimensional model to obtain better boundary condition at the toe of the dike.

After the two-dimensional calculation, the one-dimensional model is calibrated to be able to reproduce the wave spectrum at the toe of the dike. The result of the calibration is shown in Figure 10. The spectrum obtained from the two-dimensional model is now reproduced by the one-dimensional model well.

The one-dimensional model gives the wave overtopping discharge. The wave overtopping result is shown in Table 8. The wave overtopping discharge is 1.2 l/s/m whereas the wave overtopping discharge from the in-situ measurement is 0.9 l/s/m. It seems the model reproduces the wave overtopping discharge very well. However, the number of the wave overtopping is different: the number of the wave overtopping is 5 times/20 minutes whereas the wave overtopping discharge from the in-situ measurement is 25 times/20 minutes. This difference has to be investigated further in the future study.

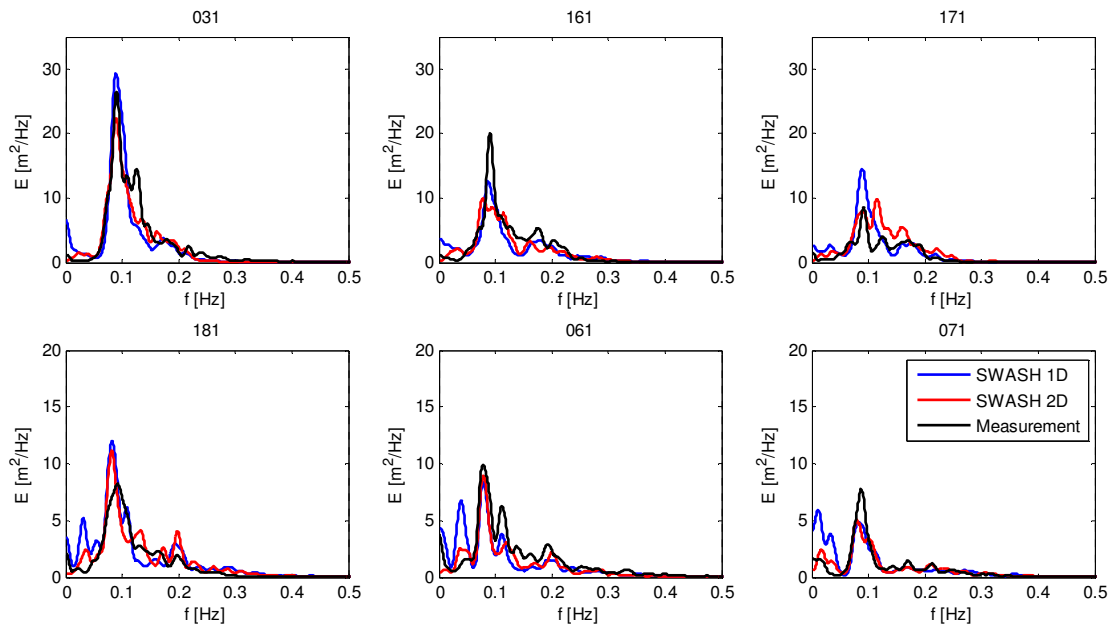


Figure 9. Computed wave spectrum by SWASH 1D (blue) and SWASH 2D (red) against in-situ measurement (black).

Conditions	Dx	H _{m0} at 071	Number of overtopping	Overtopping
[-]	[m]	[m]	[times/20 min]	[l/m/s]
SWASH 1D	2.0	2.77	0	0.0
SWASH 2D	2.0	2.46	0	0.0
In-situ measurement	-	2.54	25	0.9

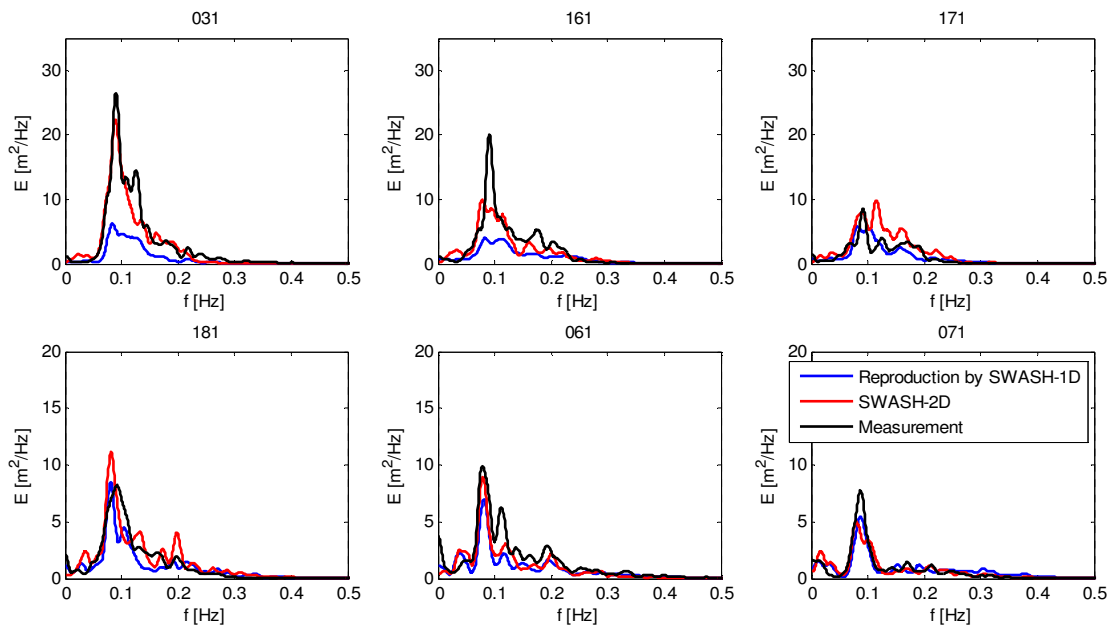


Figure 10. Comparison of the wave spectrum for different directional spreading.

Table 8. The wave overtopping discharge in different bottom frictions				
Conditions	Dx	H _{m0} at 071	Number of overtopping	Overtopping
[-]	[m]	[m]	[times/20 min]	[l/m/s]
SWASH 2D + SWASH 1D	2D: 2.0, 1D: 0.5	2.46, 2.49	5	1.2
In-situ measurement	-	2.54	25	0.9

CONCLUSIONS

The SWASH numerical model has been applied to study the wave overtopping in shallow foreshores. The key conclusions from this study are summarized as follows.

- The first-order wave generation and the second-order wave generation give significantly different wave propagation and wave overtopping.
- To choose appropriate time window is somewhat important. The first large wave group gives high overtopping discharge since the bottom is dry.
- Grid size gives a big influence on the wave overtopping discharge while wave transformation is not so sensitive to the grid size.
- Bottom friction value gives an influence on the wave overtopping discharge.
- Due to the stability of the computation, the desired calculation could not be achieved, but an alternative way to calculate wave overtopping including two-dimensional effects is proposed.

ACKNOWLEDGMENTS

The data on the prototype measurements at the Petten Sea defence are provided by Rijkswaterstaat. The data provisions are gratefully acknowledged.

REFERENCES

Barthel, V., Mansard, E. P. D., Sand, S. E. and Vis, F. C. (1983). Group bounded long waves in physical models. *Ocean Engng*, Vol. 10, No. 4, pp. 261-294.

- EurOtop. (2007) *Wave Overtopping of Sea Defences and Related Structures: Assessment Manual*, Environment Agency UK/Expertise Netwerk Waterkeren NL/Kuratorium für Forschung im Küsteningenieurwesen DE. 2007.
- Guza, R. T., and Feddersen, F. (2012). Effect of wave frequency and directional spread on shoreline runup. *Geophysical Research Letters*, 39(11).
- Mase, H., Tamada, T., Yasuda, T., Hedges, T., and Reis, M. (2013). "Wave Runup and Overtopping at Seawalls Built on Land and in Very Shallow Water." *J. Waterway, Port, Coastal, Ocean Eng.*, 139(5), 346–357.
- Ottesen Hansen, N. E., Sand, S. E., Lundgren, H., Sorensen, T., Gravesen, H. (1980). Correct reproduction of group-induced long waves. *Proceedings of the 17th Coastal Engineering Conference*, ASCE, Vol 1: 784-800.
- Rijnsdorp, D., Smit, P. B. and Zijlema, M. (2014) Non-hydrostatic modelling of infragravity waves under laboratory conditions. *Coast. Engng.*, 85, 30-42.
- Smit, P., Janssen, T., Holthuijsen, L. and Smith, J. (2014) Non-hydrostatic modeling of surf zone wave dynamics. *Coastal Engineering* 83: 36-48.
- Suzuki, T., Verwaest, T., Hassan, W., Veale, W., Reyns, J., Trouw, K., Troch, P. and Zijlema, M. (2011) The applicability of SWASH for modelling wave transformation and wave overtopping: A case study for the Flemish coast. *Proceedings in ACOMEN 2011*.
- Suzuki, T.; Gruwez, V.; Bolle, A.; Verwaest, T. (2012). Wave penetration into a shallow marina - case study for Blankenberge in Belgium, *Book of abstracts of the 4th International Conference on the Application of Physical Modelling to Port and Coastal Protection - Coastlab12*. Ghent University, Ghent, Belgium, September 17-20, 2012. pp. 135-136
- Van Gent, M. R. A. (1999). *Physical model investigations on coastal structures with shallow foreshore: 2D model tests with single and double-peaked wave energy spectra*. WL | Delft Hydraulics.
- Williams, E., Briganti, R., Pullen, T. (2014). The role of offshore boundary conditions in the uncertainty of numerical prediction of wave overtopping using non-linear shallow water equations, *Coastal Engineering*, 89: 30-44.
- Zijlema, M., Stelling, G.S. and Smit P. (2011) SWASH: An operational public domain code for simulating wave fields and rapidly varied flows in coastal waters. *Coastal Engineering*, 58: 992-1012.